Calculations of kaonic nuclei based on chiral meson-baryon coupled channel interaction models

J. Hrtánková, J. Mareš

Nuclear Physics Institute, Řež, Czech Republic

55th International Winter Meeting on Nuclear Physics
Bormio, January 23 - 27, 2017

Introduction

- Interactions between K^- and nucleon(s) is topical but still not resolved problem
- Existence of the $I = 0$ $\pi\Sigma$ resonance $\Lambda(1405)$ below K^-N threshold
  $\rightarrow$ K^-N interaction attractive + strongly coupled to $\pi\Sigma$ channel
  $\rightarrow$ strong K^- absorption
- Are there any (narrow) deeply bound K^--nucler states?
  – no decisive answer so far

Introduction

- Self-consistent calculations of K^--nuclear quasi-bound states using the following chiral meson-baryon interaction models:
  - Prague (P)
    (A. Cieply, J. Smejkal, Nucl. Phys. A 881 (2012) 115)
  - Kyoto-Munich (KM)
    (Y. Ikeda, T. Hyodo and W. Weise, Nucl. Phys. A 881 (2012) 98)
  - Murcia (M1 and M2)
    (Z. H. Guo and J. A. Oller, Phys. Rev. C 87 (2013) 035202)
  - Bonn (B2 and B4)
    (M. Mai and U.-G. Meißner, Nucl. Phys. A 900 (2013) 51)

Free-space K^-p amplitudes

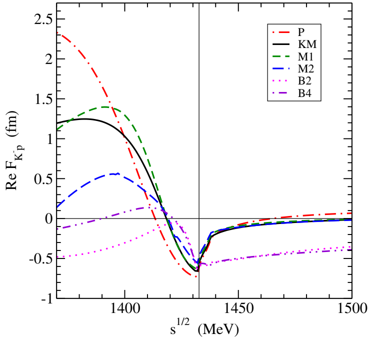

Fig.1: Energy dependence of real (left) and imaginary (right) parts of free-space K^-p amplitudes in considered models.

Free-space $K^- n$ amplitudes

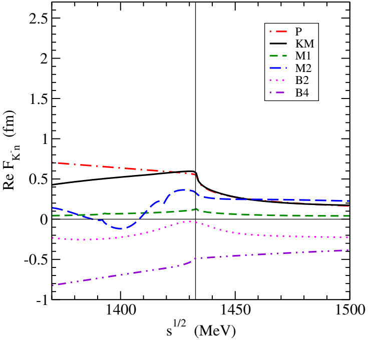

Fig.2:Energy dependence of real (left) and imaginary (right) parts of free-space $K^- n$ amplitudes in considered models.

Model

- Klein-Gordon equation for K^-

$$\left[\tilde{\omega}_K^2 + \vec{\nabla}^2 - m_K^2 - \Pi_K(\vec{p}_K, \omega_K, \rho)\right] \phi_K = 0$$

complex energy $\tilde{\omega}_K = m_K - B_K - \mathrm{i}\Gamma_K/2 - V_C = \omega_K - V_C$

- Self-energy operator

$$\Pi_K = 2\mathrm{Re}(\omega_{K^-}) V_{K^-}^{(1)} = -4\pi \frac{\sqrt{s}}{m_N} \left(F_0 \tfrac{1}{2}\rho_p + F_1 \left(\tfrac{1}{2}\rho_p + \rho_n\right)\right),$$

F_0 and F_1 – isospin 0 and 1 scattering amplitudes from a chiral meson-baryon interaction model

- Nucleus described within an RMF model
- Static self-consistent calculations — core polarization effect up to $\simeq 5$ MeV in K^- binding energies
(D. Gazda, J. Mareš, Nucl. Phys. A 881, 159 (2012))

Model

- Free space amplitudes $\to$ in-medium amplitudes - WRW method
  (T. Wass, M. Rho, W. Weise, Nucl. Phys. A 617 (1997) 449)

$$F_1 = \frac{F_{K^-n}(\sqrt{s})}{1 + \frac{1}{4}\xi_k \frac{\sqrt{s}}{m_N} F_{K^-n}(\sqrt{s})\rho}\,, \qquad F_0 = \frac{[2F_{K^-p}(\sqrt{s}) - F_{K^-n}(\sqrt{s})]}{1 + \frac{1}{4}\xi_k \frac{\sqrt{s}}{m_N}[2F_{K^-p}(\sqrt{s}) - F_{K^-n}(\sqrt{s})]\rho}$$

where

$$\xi_k = \frac{9\pi}{p_f^2} 4\int_0^\infty \frac{dt}{t} \exp(iqt) j_1^2(t), \qquad q = \frac{1}{p_f}\sqrt{{\omega_{K^-}}^2 - m_{K^-}^2}.$$

- P + Pauli + SE model
  (A. Cieply, J. Smejkal, Nucl. Phys. A 881 (2012) 115)

$$F_{ij}(p, p^{'}; \sqrt{s}) = -\frac{g_i(p) g_j(p^{'})}{4\pi f_i f_j}\sqrt{\frac{M_i M_j}{s}}\left[(1 - C(\sqrt{s}) \cdot G(\sqrt{s})^{-1}) \cdot C(\sqrt{s})\right]_{ij}\,,$$

$$G_i(\sqrt{s}; \rho) = \frac{1}{f_i^2}\frac{M_i}{\sqrt{s}}\int_{\Omega_i(\rho)} \frac{d^3\vec{p}}{(2\pi)^3}\frac{g_i^2(p)}{p_i^2 - p^2 - \Pi_i(\sqrt{s}, \vec{p}; \rho) + i0}\,.$$

In-medium modified $\bar{K}N$ amplitudes

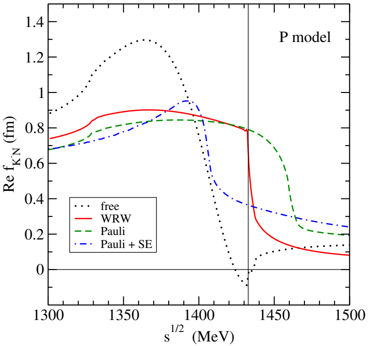

Fig.3: Energy dependence of reduced free-space (dotted line) $f_{\bar{K}N} = \frac{1}{2}(f_{K^-p} + f_{K^-n})$ amplitude compared with WRW modified amplitude (solid line), Pauli (dashed line), and Pauli + SE (dot-dashed line) modified amplitude for $\rho_0 = 0.17\ \mathrm{fm}^{-3}$ in the P model.

Energy dependence

- K^-N amplitudes are a function of $\sqrt{s}$
  $(s = (E_N + E_{K^-})^2 - (\vec{p}_N + \vec{p}_{K^-})^2)$
- K^-N cms frame $\rightarrow$ K^--nucleus frame $\vec{p}_N + \vec{p}_{K^-} \neq 0$
  (A. Cieplý, E. Friedman, A. Gal, D. Gazda, J. Mareš PLB 702 (2011) 402)
- Low-density limit $\delta\sqrt{s} \rightarrow 0$ as $\rho \rightarrow 0$ where $\delta\sqrt{s} = \sqrt{s} - E_{th}$

$$\sqrt{s} = E_{th} - B_N \frac{\rho}{\bar{\rho}} - \xi_N \left[B_{K^-} \frac{\rho}{\rho_{max}} + 23 \left(\frac{\rho}{\bar{\rho}} \right)^{2/3} + V_C \left(\frac{\rho}{\rho_{max}} \right)^{1/3} \right] + \xi_{K^-} \mathrm{Re} V_{K^-}(r) \ ,$$

where $B_N = 8.5$ MeV and $\xi_{N(K^-)} = m_{N(K^-)}/(m_N + m_{K^-})$.

Energies probed in the calculations

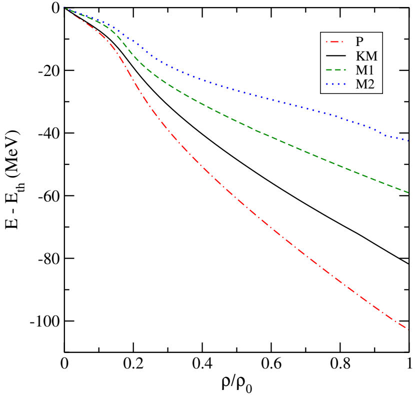

Fig.4: Subthreshold energies probed in the $^{16}O+K^-$ nucleus as a function of relative density ρ/ρ_0, calculated self-consistently using K^-N amplitudes in the P, KM, M1, and M2 models.

K^- 1s binding energies and widths

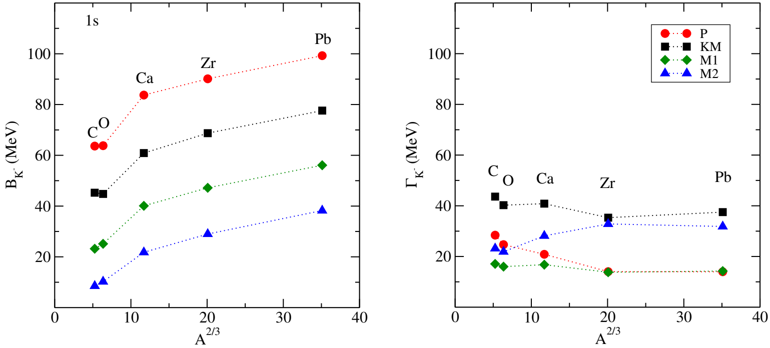

Fig.5: 1s K^- binding energies (left) and corresponding widths (right) in various nuclei calculated self-consistently in the P, KM, M1, and M2 models.

Multinucleon processes

- K^- interactions with two and more nucleons - recent analysis of kaonic atom data including branching ratios of K^- absorption by Friedman and Gal (*NPA 959 (2017) 66*)

$$2\mathrm{Re}(\omega_{K^-})V^{(2)}_{K^-} = -4\pi B(\frac{\rho}{\rho_0})^\alpha \rho \ , \qquad (1)$$

where B is a complex amplitude and α is positive

- Only P and KM models preferred by the analysis (P1, KM1 for $\alpha = 1$ and P2, KM2 for $\alpha = 2$)
- $K^-NN \rightarrow \Sigma N$ – dominant K^- absorption mode in the nuclear interior $\rightarrow$ ImB multiplied by a kinematical suppression factor $f_{\Sigma N}$

Multinucleon processes

- Total K^- optical potential $V_{K^-} = V_{K^-}^{(1)} + V_{K^-}^{(2)}$
- Experiments with kaonic atoms probe the K^- optical potential (mainly its imaginary part) up to $\sim 50\%$ of ρ_0
- We consider two limiting cases for $V_{K^-}^{(2)}$ in our calculations
  - form (1) in the entire nucleus – full density option (FD)
  - fix $V_{K^-}^{(2)}$ at constant value $V_{K^-}^{(2)}(0.5\rho_0)$ for $\rho(r) \geq 0.5\rho_0$ – half density limit (HD)

Total K^- optical potential

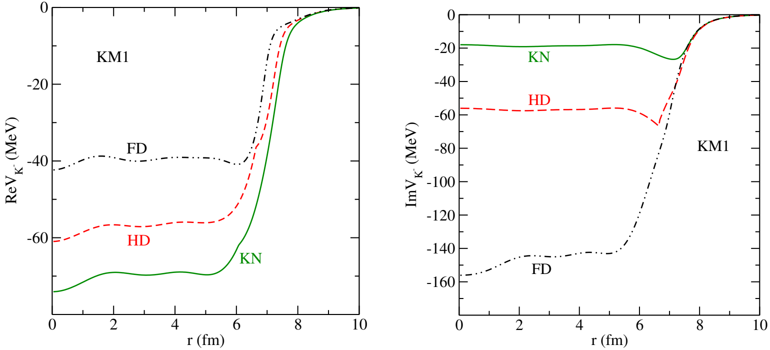

Fig.6: The real and imaginary parts of the K^- optical potential in the ^{208}Pb+K^- nucleus, calculated self-consistently in the KM1 model for two versions of the K^- multinucleon potential. The single-nucleon K^- potential (green solid line) calculated in the corresponding model is shown for comparison.

Contributions to the total K^- optical potential

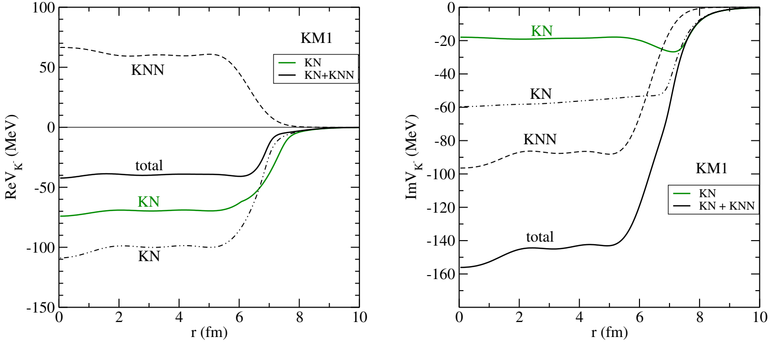

Fig.7: The respective contributions from K^-N and K^-NN potentials to the total real and imaginary K^- optical potential in the ^{208}Pb+K^- nucleus, calculated self-consistently in the KM1 model and FD variant. The single-nucleon K^- potential (green solid line) calculated in the corresponding model is shown for comparison.

K^- 1s binding energies and widths

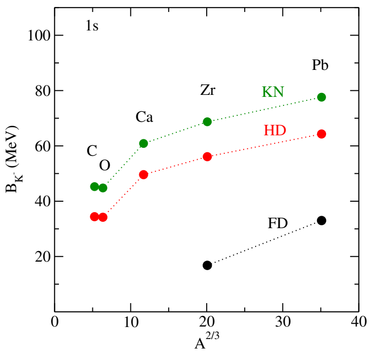

Fig.8: 1s K^- binding energies (left) and corresponding widths (right) in various nuclei calculated self-consistently for two options of $V_{K^-}^{(2)}$ in the KM1 model.

Ratios of K^- absorption in medium

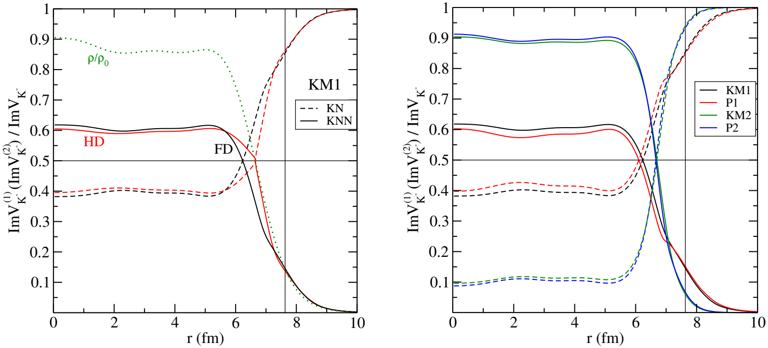

Fig.9: Ratios of $\mathrm{Im}\,V_{K^-}^{(1)}$ and $\mathrm{Im}\,V_{K^-}^{(2)}$ potentials to the total K^- imaginary potential $\mathrm{Im}\,V_{K^-}$ as a function of radius, calculated self-consistently for ^{208}Pb$+K^-$ system in the KM1 model and different option for the K^- multinucleon potential (left) and the comparison of these ratios calculated in different meson-baryon interaction models for FD option (right). The vertical lines denoting $\sim 15\%$ of ρ_0 are shown for comparison.

Conclusions

- Calculations of K^--nuclear quasi-bound states in various nuclei
- K^- single-nucleon potentials based on chiral meson-baryon interaction models yield:
  - large model dependence of K^- binding energies
  - small K^- widths
- Sizeable contribution from K^- multinucleon interactions inside the nucleus:
  - K^- widths significantly larger than binding energies, if ever bound

Thank you for your attention!

backup slides

K^- optical potential

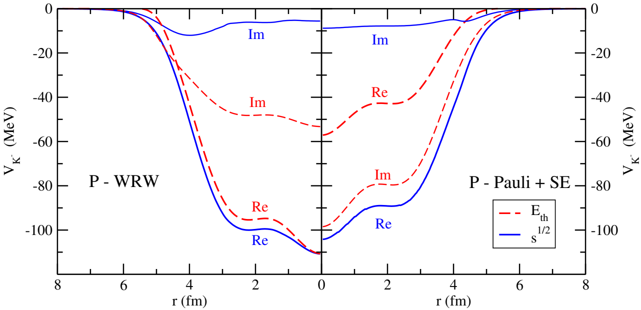

Fig.10: K^- optical potential in ^{40}Ca calculated self-consistently for in-medium $\sqrt{s}$ and at threshold E_{th} using WRW modified amplitudes in the P NLO model compared with P NLO + Pauli + SE model.

K^- optical potential

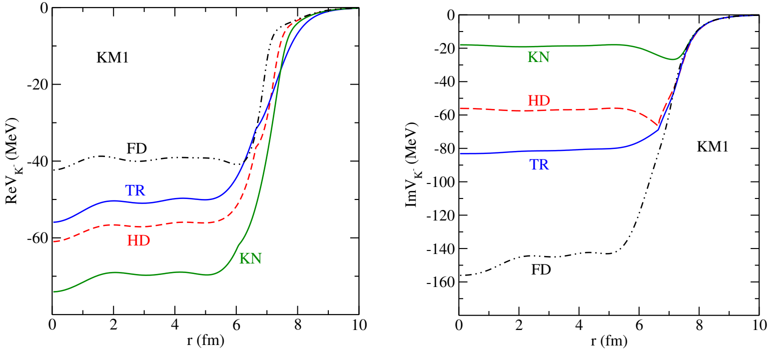

Fig.11: 1s K^- binding energies (left) and corresponding widths (right) in various nuclei calculated self-consistently for different options of $V_{K^-}^{(2)}$ in the KM1 model.

K^- 1s binding energies and widths

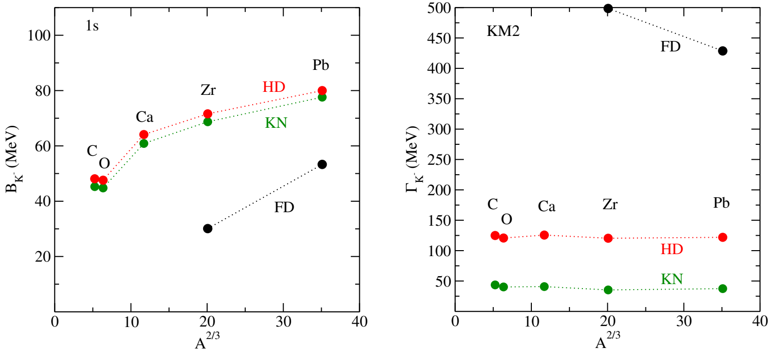

Fig.12: 1s K^- binding energies (left) and corresponding widths (right) in various nuclei calculated self-consistently for two options of $V^{(2)}_{K^-}$ in the KM2 model.

Multinucleon processes

Table : Values of the complex amplitude B and exponent α used to evaluate $V_{K^-}^{(2)}$ for all chiral meson-baryon interaction models considered in this work.

	B2	B4	M1	M2	P1	KM1	P2	KM2
α	0.3	0.3	0.3	1	1	1	2	2
ReB (fm)	2.4	3.1	0.3	2.1	-1.3	-0.9	-0.5	0.3
ImB (fm)	0.8	0.8	0.8	1.2	1.5	1.4	4.6	3.8